IOP Conference Series: Earth and Environmental Science

PAPER • **OPEN ACCESS**

Three-objective optimization of a single-channel pump for wastewater treatment

IOP Conf. Series: Earth and Environmental Science **240** (2019) 032010 doi:10.1088/1755-1315/240/3/032010

Three-objective optimization of a single-channel pump for wastewater treatment

Jin-Hyuk Kim[1, 2], Wang-Gi Song[1, 2], Young-Seok Choi[1, 2], Kyoung-Yong Lee[1], Sang-Bum Ma[3] and Kwang-Yong Kim[3]

[1] Thermal & Fluid System R&D Group, Korea Institute of Industrial Technology, Cheonan 31056, Republic of Korea
[2] Advanced Energy & Technology, University of Science & Technology, Daejeon 34113, Republic of Korea
[3] Department of Mechanical Engineering, Inha University, Incheon 22212, Republic of Korea

jinhyuk@kitech.re.kr

Abstract. The impeller and volute of a single-channel pump used for wastewater treatment were simultaneously optimized to improve the hydraulic efficiency and reduce unsteady radial force sources due to the impeller–volute interaction. Steady and unsteady Reynolds-averaged Navier–Stokes equations were solved with the shear stress transport turbulence model as the turbulence closure model using tetrahedral grids to analyze the internal flow in the single-channel pump. Five design variables related to the internal flow cross-sectional areas of the impeller and volute were selected to simultaneously optimize the hydraulic efficiency, the sweep area of the radial force during one revolution, and the distance of the mass center of the sweep area from the origin as the three objective functions. The response surface approximation model and genetic algorithm were employed to obtain three-dimensional Pareto-optimal solutions representing the trade-off between the efficiency and the radial force sources. The results of the three-objective optimization show that the representative clustered optimum designs enhanced the efficiency and reduced the radial force sources simultaneously in most cases, compared to the reference design. In addition, it was confirmed that the trade-off between the efficiency and the radial force sources clarifies with controlling the internal flow cross-sectional areas of the impeller and volute of the single-channel pump.

1. Introduction

Lately, the demand for a submerged pump with a wide flow path is rapidly increasing in the field of wastewater treatment. This is because the most common fault in submerged pumps is waste clogging. As the single-channel pump is a representative case of the wide flow path pump, it can be smoothly driven in various sewages containing solid wastes because the single-channel impeller has only one free annulus passage. Hence, a single-channel pump is very robust, particularly against damage and failure due to waste clogging.

Nevertheless, only a few studies have been conducted on the design technology of a single-channel pump [1, 2], because of the difficulties in establishing a theoretical design methodology and other manufacturing problems. Moreover, it is particularly difficult to solve the balancing problem related to the fluid-induced vibration due to the interaction between the rotating impeller and the stationary volute. In fact, as the mass distribution of a single-channel impeller is rotationally unsymmetrical, it is difficult to stabilize the unsteady flow-induced vibration due to the interaction between the rotating impeller and the stationary volute. Moreover, unsteady radial forces, the frequency of rotation of which depends on the rotating speed, are generated in the single-channel impeller [3]. The unsteady sources are due to the interaction between the rotating impeller and the stationary volute. They adversely affect the overall system of the single-channel pump, particularly in terms of the life expectancy and durability of the pump.

Recently the authors proposed a theoretical approach for designing the impeller and volute of a single-channel pump and attempted to optimize the hydraulic efficiency and reduce the unsteady radial force sources. However, the impeller and volute shapes were not optimized simultaneously from a practical perspective. Therefore, the unsteady flow-induced vibration due to the interaction between the rotating impeller and the stationary volute could not be analyzed systematically.

This paper presents a simultaneous three-objective optimization technique to improve the hydraulic efficiency and reduce the unsteady radial force sources due to the impeller–volute interaction considering both the impeller and volute shapes of a single-channel pump used for wastewater treatment. The aim of this study is to provide a practical guideline for designing single-channel pumps with high efficiency and less fluid-induced vibration.

2. Design approach for a single-channel pump model

The initial concept of the single-channel impeller and volute is based on the Stepanoff theory outlined in previous studies [4-6]. The pump can then be modeled as a three-dimensional shape, as shown in figure 1 [7]. Thus, the initial shapes of the impeller and volute have area distributions that constantly increase with an increase in the angle theta between the impeller and the volute, from the inlet to the outlet, as shown in figure 2. Although the Stepanoff theory is generally used to design the stationary volute, it was employed for designing both the impeller and volute because they each have only one free annulus passage. The flow ($\Phi = Q/ND^3$) and head ($\psi = gH/N^2D^2$) coefficients for the reference single-channel pump model are 0.019 and 0.074, respectively. Here, Q, N, D, g, and H denote the volume flow rate, rotational speed, impeller diameter, acceleration due to gravity, and total head, respectively.

3. Steady and unsteady numerical analyses

In the computation domain generated from the basic design approach, the internal flow field was

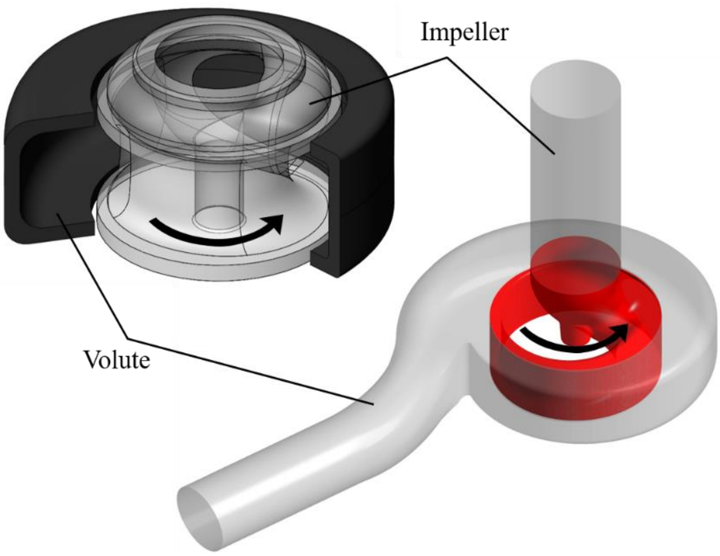

Figure 1. Three-dimensional shape of a single-channel pump [7].

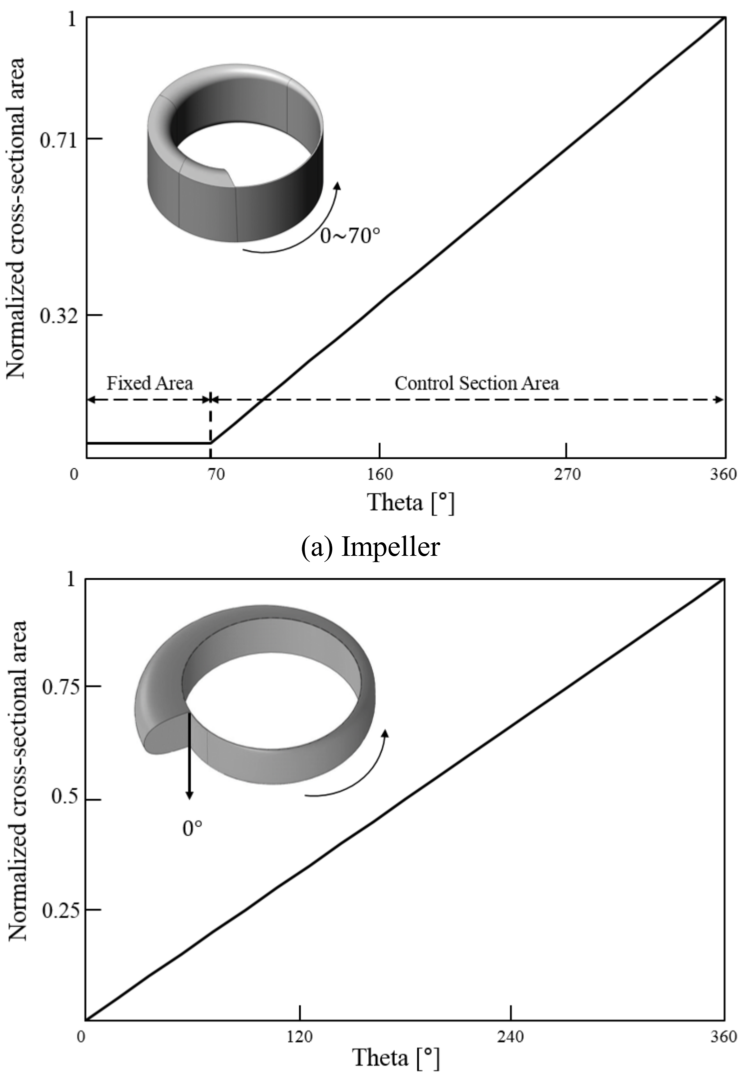

Figure 2. Cross-sectional area distributions of a) impeller and b) volute.

analyzed by solving the three-dimensional steady and unsteady incompressible Reynolds-averaged Navier–Stokes (RANS) equations with a k-ω-based shear stress transport (SST) turbulence model using a finite volume solver provided in the commercial code ANSYS CFX-14.5.

A tetrahedral grid system was constructed in the computational domain with a prism mesh near the surfaces. The rotating single-channel impeller and the volute domains were constructed using approximately 1,300,000 and 1,200,000 grid points, respectively. Hence, the optimum grid system selected using the grid independency test has approximately 2,500,000 grid points, as previously reported [5].

For the boundary condition, water was considered as the working fluid, and the total pressure and designed mass flow rate were set to the inlet and outlet of the computational domain, respectively. The solid surfaces in the computational domain were considered hydraulically smooth under adiabatic and no-slip conditions. The stage average and transient-rotor-stator methods were respectively applied to connect the interface between the rotating impeller and the volute domains in the steady and unsteady analyses.

The convergence criteria in the steady computation consisted of the root-mean-square (RMS) values of the residuals of the governing equations; the values were set lower than 10^{-5} for all equations. The

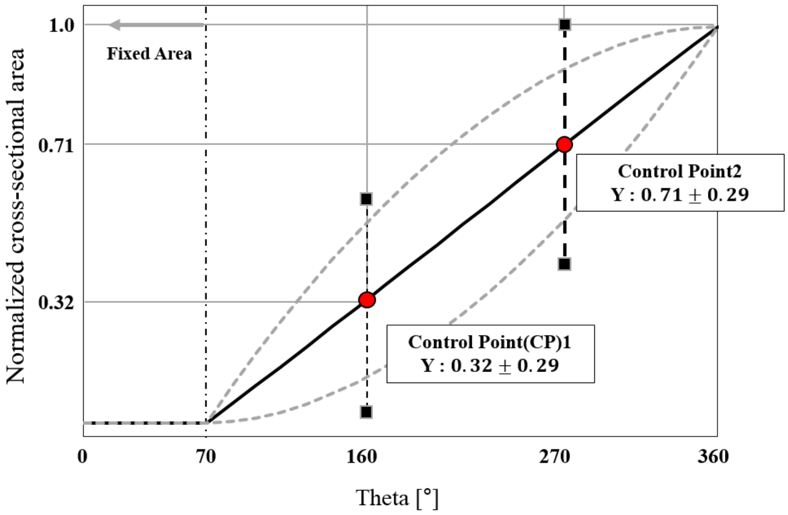

(a) Impeller

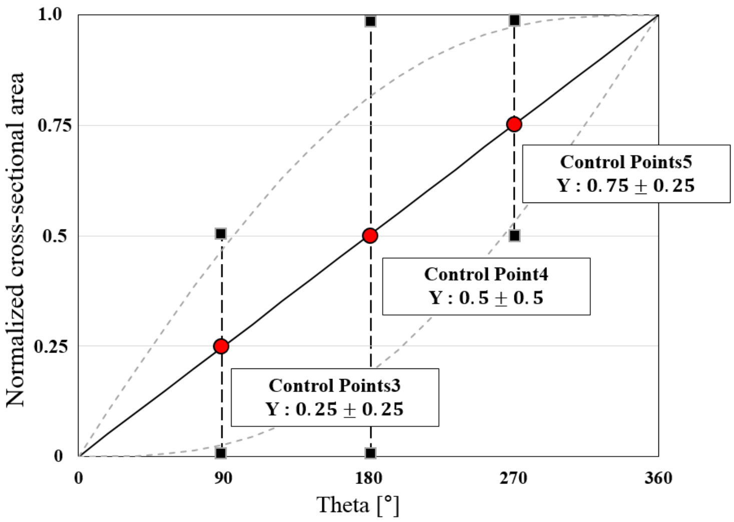

(b) Volute

Figure 3. Definition of the design variables.

physical time scale was set to 1/ω, where ω is the angular velocity of the impeller. The computations were conducted using an Intel Xeon CPU with a clock speed of 2.70 GHz, and the converged solutions are obtained after 1,000 iterations with a computational time of approximately 4 h.

The results of the steady RANS analysis were used for the unsteady RANS analysis to obtain the characteristics of the radial force sources in the region near the exit surface of the impeller, on the basis of the impeller–volute interactions in the single-channel pump. In the unsteady computations, the time step and the coefficient loop for the time-scale control were set to 0.000947 s and three times, respectively. The solutions were obtained after 180 iterations with an unsteady total time duration of 0.1704775 s (five revolutions), and the computational time required for the unsteady calculation was 8 h.

4. Optimization techniques

In this work, the geometric parameters related to the internal flow through the cross-sectional areas of the impeller and volute were selected as the design variables to simultaneously optimize the hydraulic efficiency and radial force sources, considering the interaction between the rotating impeller and the stationary volute of a single-channel pump. The internal flow distributions at the cross-sectional area of the impeller and volute can be changed smoothly by adjusting the control points represented by third-order and fourth-order Bezier curves, respectively, as shown in figure 3. Therefore, the variations in the five control points (CP1, CP2, CP3, CP4, and CP5) along the *y*-axes for both the impeller and volute were selected as the design variables to obtain the most sensitive results for the variation in the curve among the control points [6].

The objective of the current optimization problem was to simultaneously improve the hydraulic efficiency (η) and reduce the radial force sources considering the impeller–volute interaction in the single-channel pump. Here, one of the three objective functions, i.e., the hydraulic efficiency, is defined as follows.

$$\eta = \frac{\rho g H Q}{\tau \omega} \tag{1}$$

where ρ, τ, and ω denote the density, torque, and angular velocity, respectively.

The other objective functions related to the radial force sources are the sweep area (As) of the radial force during one revolution of the impeller and the distance (Ds) of the mass center of the sweep area from the origin, as shown in figure 4 [7]. These functions are defined as follows.

$$A_s = \frac{1}{2}\sum_{i=0}^{n-1}(x_i y_{i+1} - x_{i+1} y_i) \tag{2}$$

where A_s is the area of the polygon selected as the sweep area of the radial force during one revolution of the impeller. The centroid of a non-self-intersecting closed polygon, defined by n vertices (x_0, y_0), (x_1, y_1),..., (x_{n-1}, y_{n-1}), is defined as point (C_x, C_y) as follows.

$$C_x = \frac{1}{6A_s}\sum_{i=0}^{n-1}(x_i + x_{i+1})(x_i y_{i+1} - x_{i+1} y_i) \tag{3}$$

$$C_y = \frac{1}{6A_s}\sum_{i=0}^{n-1}(y_i + y_{i+1})(x_i y_{i+1} - x_{i+1} y_i) \tag{4}$$

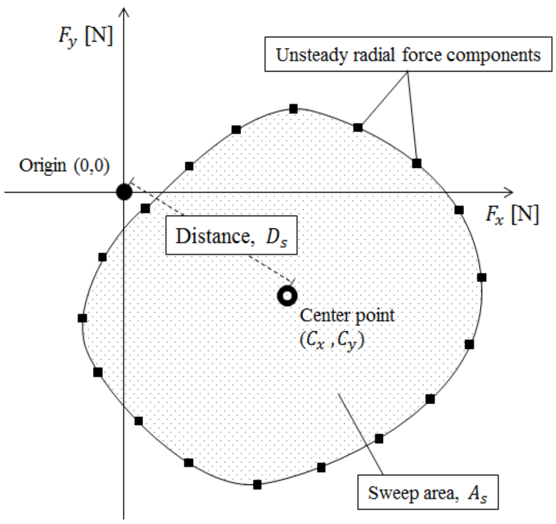

Figure 4. Definition of objective functions related to the radial force sources [7].

In the formulae, the vertices are assumed to be numbered in the order of their occurrences along the perimeter of the polygon. Therefore, the distance of the mass center of the sweep area from the origin can be defined as follows.

$$D_s = \sqrt{{C_x}^2 + {C_y}^2} \tag{5}$$

The Latin hypercube sampling (LHS) [8] was employed to generate 54 design points, which are used as the initial base data for constructing the response surface from the five design variables. The RSA models were employed to construct the response surfaces based on the objective function values at the 54 design points generated in the design space using LHS. A hybrid multi-objective genetic algorithm (MOGA) was used to obtain the global Pareto-optimal solutions (POSs). The approximate POSs were obtained using a controlled elitist genetic algorithm (a variant of NSGA-II [9]) as the MOGA functions for the three objective functions. The optimization algorithm and the functions in the MATLAB OPTIMIZATION TOOLBOX [10] were used to finally generate the global POSs.

5. Results and discussion

To evaluate the accuracy and validity of the numerical analysis conducted in this work, the results of the flow analysis should be verified prior to the optimization. In previous studies [11-13], the accuracy of the numerical analysis conducted on a single-channel pump has been evaluated by validating the results of the steady-state flow analysis by comparing them to the experimental data.

A hybrid MOGA based on the response surface constructed from the RSA model was employed to obtain the global POSs using a controlled elitist genetic algorithm (a variant of NSGA-II) for the three objective functions. Here, the functional forms of the RSA models for the three objective function values in terms of the design variables normalized between 0 and 1 can be expressed as follows.

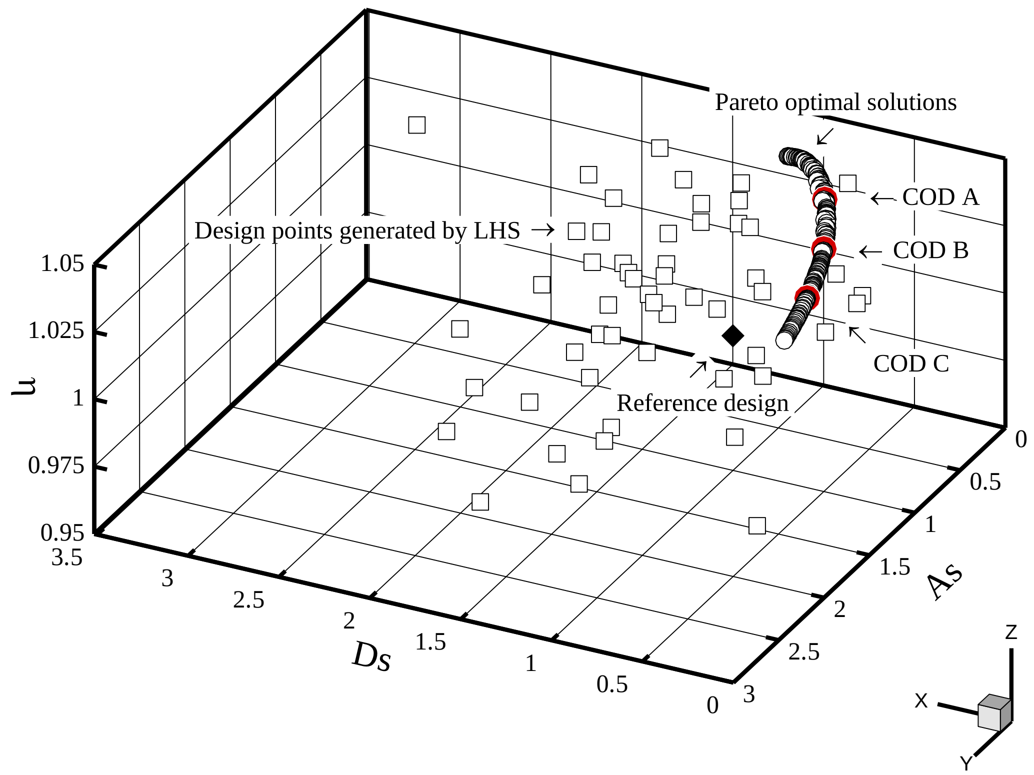

Figure 5. Results of the three-objective optimization.

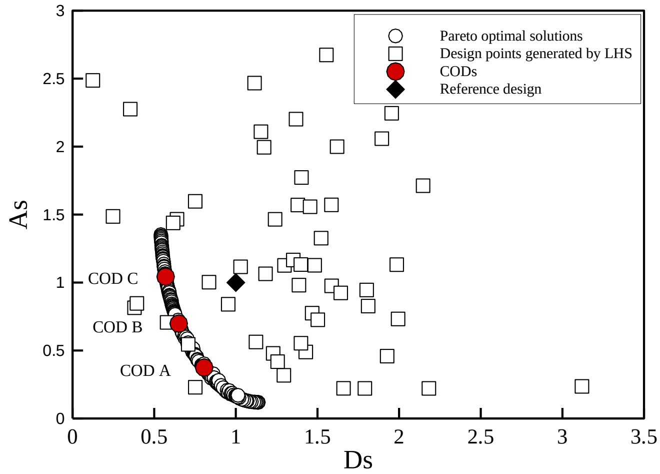

(a) Ds-As

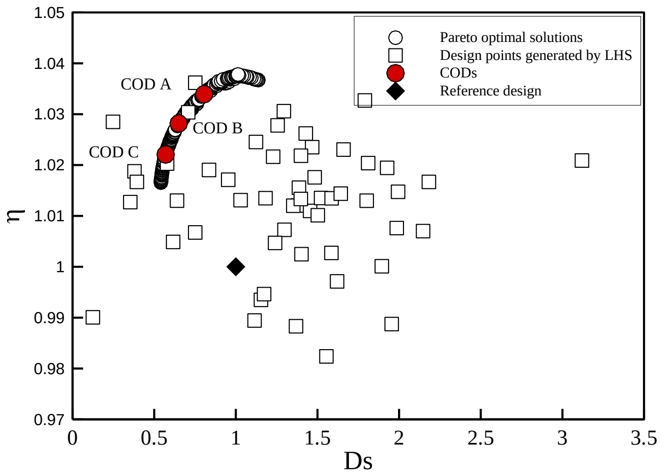

(b) Ds-Eff

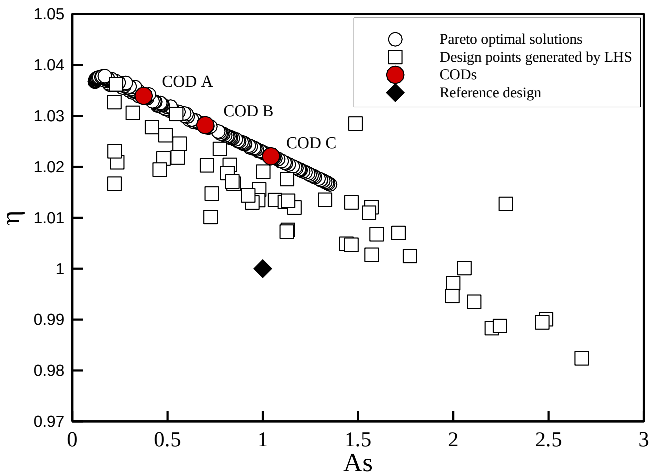

(c) As-Eff

Figure 6. Results of POSs in two-dimensional functional space.

Table 1. Results of three-objective optimization with clustered optimum points.

Designs	Hybrid MOGA			(U)RANS			Increment (compared to ref)		
	η	*As*	*Ds*	η	*As*	*Ds*	η	*As*	*Ds*
Ref	-	-	-	1.000	1.000	1.000	-	-	-
COD A	1.034	0.375	0.806	1.034	0.297	0.700	0.034	−0.703	−0.300
COD B	1.028	0.698	0.650	1.027	0.697	0.601	0.027	−0.303	−0.399
COD C	1.022	1.043	0.570	1.019	1.050	0.596	0.019	0.050	−0.404

$$\eta = -81.9431-1.647x_1+0.289252x_2+0.156913x_3-0.0041x_4-1.60471x_5+0.601399x_1x_2-0.28871x_1x_3 +0.139474x_1x_4+0.137328x_1x_5+0.395176x_2x_3+0.260511x_2x_4+1.138769x_2x_5-0.37491x_3x_4 +0.766416x_3x_5-0.19393x_4x_5+3.180764x_1^2+0.361327x_2^2+0.072956x_3^2+0.570979x_4^2+0.59507x_5^2 \quad (6)$$

$$As = 25503.35-21658.6x_1+69962.69x_2-9888.18x_3-21104.1x_4-575.057x_5+16430.47x_1x_2 +2870.249x_1x_3-12186.2x_1x_4+1425.672x_1x_5+465.6003x_2x_3+9526.738x_2x_4-5860.78x_2x_5-10720.5x_3x_4 +19390.96x_3x_5+4238.049x_4x_5+134526.2x_1^2+24891.4x_2^2+1070.46x_3^2+24231.77x_4^2-11071.1x_5^2 \quad (7)$$

$$Ds = 55.99863-41.6106x_1-27.9953x_2+16.18584x_3-47.0416x_4-34.9683x_5-3.62163x_1x_2+16.57149x_1x_3 +29.75539x_1x_4-0.83978x_1x_5+1.257038x_2x_3-9.40075x_2x_4+8.368733x_2x_5-15.6539x_3x_4-31.8108x_3x_5 +19.89881x_4x_5+25.41738x_1^2+24.76387x_2^2+30.06504x_3^2+44.09973x_4^2+22.35891x_5^2 \quad (8)$$

where x_1–x_5 represent the normalized design variables corresponding to the five control points.

Figure 5 shows the results of the three-dimensional POSs with respect to the three objective functions obtained using the hybrid MOGA combined with the RSA model. Here, the values of all the objective functions were normalized based on the corresponding values in the reference design. As shown in figure 5, the three-dimensional POSs are clearly the trade-off among the conflicting objective functions. A trade-off analysis showed an obvious correlation between the hydraulic efficiency and the radial force sources.

Figure 6 shows the trade-off of the POSs in each two-dimensional functional space to more clearly understand the optimization results. As shown in figures 6(a) and (b), the decrement in the distance of the mass center of the sweep area from the origin clearly leads to the deterioration in the other objective functions. In particular, the reduced distance was obtained at a lower efficiency and higher sweep area of the radial force during one revolution. However, the efficiency and sweep area of the radial force during one revolution shows a positive relation, as shown in figure 6(c). In other words, a higher efficiency corresponds to a smaller sweep area of the radial force during one revolution. Therefore, the trade-off analysis of the POSs can help an engineering designer to select an economic solution depending on the required design conditions.

Table 1 lists the results of the objective functions for the three representative clustered optimum designs (CODs) with respect to the three-dimensional POSs, which are also shown in figures 5 and 6, along with the reference design. In Table 1, the objective function values predicted using the hybrid MOGA are generally quite accurate compared to the calculated steady and unsteady RANS values. Nevertheless, relatively high errors are observed in the three objective functions, particularly in the distance of the mass center of the sweep area from the origin. The calculated steady and unsteady RANS values of the three objective functions for the CODs were compared with the corresponding values of the reference design. The objective function values for all CODs are generally better than those of the reference design, except for the sweep area of the radial force during one revolution of the impeller of COD C. The results of COD A showed the highest efficiency and lowest sweep area values, and their increment and decrement were 0.034 and 0.703, respectively, compared to the corresponding values of the reference design. On the contrary, the result of COD C had the lowest distance value (0.404) in comparison to that of the reference design.

Figure 7 shows the distribution of the cross-sectional areas along with the theta angle between the impeller and volute for the reference design and CODs. The cross-sectional area distribution of the impeller of COD A, which has the highest efficiency and smallest sweep area, has the most concave shape compared to the other designs, as shown in figure 7(a). The concave flow path of the impeller was much more sensitive and important for a high-efficiency and low-sweep-area design. On the other hand, the cross-sectional area distribution of COD C with the lowest distance of the mass center of the sweep area from the origin is largely similar to that of the reference design. In figure 7(b), the cross-sectional area distributions of the volute in all CODs increase smoothly from 0° to 300° and then the slopes decrease gradually. This implies that the upstream distribution at the cross-sectional area of the

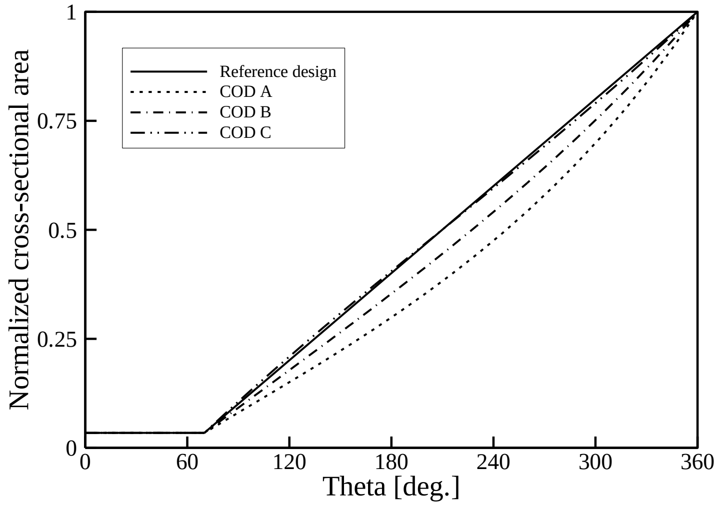

(a) Impeller

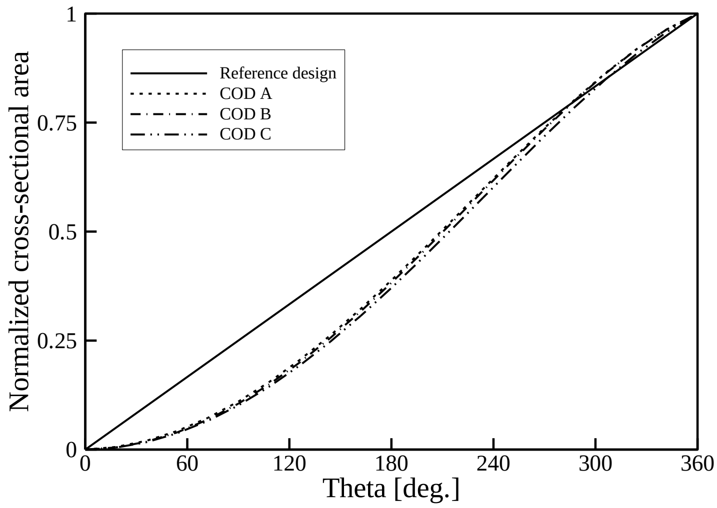

(b) Volute

Figure 7. Cross-sectional area distributions of the impeller and volute.

volute remarkably contributed to the performance enhancement of all the objective functions related to the hydraulic efficiency and radial force sources. The results show that the cross-sectional area distributions of the impeller and volute should be simultaneously considered in the design of single-channel pumps with high efficiency and less fluid-induced vibration.

6. Conclusions

The impeller and volute of a single-channel pump for wastewater treatment were simultaneously optimized using a hybrid MOGA with three-dimensional steady and unsteady RANS analyses. A three-objective optimization was simultaneously conducted to improve the hydraulic efficiency and reduce the unsteady radial force sources due to the impeller–volute interaction using five design variables related to the cross-sectional areas of the internal flow of the impeller and volute. The hydraulic efficiency, the sweep area of the radial force during one revolution, and the distance of the mass center of the sweep area from the origin were selected as the three objective functions. A trade-off analysis of the three-dimensional POSs showed an obvious correlation between the hydraulic efficiency and the radial force sources. In particular, the decrement in the distance of the mass center of the sweep area from the origin clearly led to the deterioration in the other objective functions. Moreover, the reduced distance was obtained at a lower efficiency and larger sweep area of the radial force during one revolution. However, the efficiency and the sweep area of the radial force during one revolution showed a positive relation. The cross-sectional area distributions for the three representative CODs with respect to the three-dimensional POSs were analyzed to investigate their effects on the three objective functions related to the hydraulic efficiency and unsteady radial force sources due to the impeller–volute interaction. A concave flow path for the impeller was found to be much more sensitive and important for a high-efficiency and small sweep area design, whereas a straight flow path was more sensitive for a design with the shortest distance of the mass center of the sweep area from the origin. In addition, the upstream distribution at the cross-sectional area of the volute remarkably contributed to the performance enhancement of all the objective functions related to the hydraulic efficiency and radial force sources. These results show that the cross-sectional area distributions of the impeller and volute should be simultaneously considered for designing single-channel pumps with high efficiency and less fluid-induced vibration.

Acknowledgment

This work was supported by the Demand-based-Manufacturing Technique Commercialization R&D Project of the Korea Institute of Industrial Technology (KITECH) (No. JB180001), which was funded by the Ministry of Science and ICT (MSIT). The authors gratefully acknowledge this support.

References

[1] Hansen B F and Henning P J 2013 Waste water pump US Patent Application No. 13 886,479
[2] Pei J, Benra F K and Dohmen H J 2012 Application of different strategies of partitioned fluid–structure interaction simulation for a single-blade pump impeller *Proc IMechE Part E: J Process Mechanical Engineering* **226** 4
[3] Gulich J F 2008 *Centrifugal pumps* (Verlag Berlin Heidelberg: Springer)
[4] Cho B M, Kim J H, Choi Y S, Lee K Y, Oh H Y, Kim K Y, Kim Y S and Kim J H 2015 High-efficiency design technique of a single-channel submersible pump impeller for waste treatment *ASME-JSME-KSME Joint Fluids Engineering* AJKFluids2015-09203
[5] Kim J H, Cho B M, Choi Y S and Lee K Y 2016 Multi-objective optimization based on unsteady analysis considering the efficiency and radial force of a single-channel pump for wastewater treatment *J Mechanics Engineering and Automation* **6** 5
[6] Cho B M, Kim J H, Choi Y S, Kim J W, Kim Y S, Kim K Y, Ahn T S and Kim J H 2015 Surrogate based optimization of a single-channel pump impeller *7th International Conference on Pumps and Fans 2015* ICPF-121
[7] Cho B M 2017 A study on numerical optimization of flow path cross-sectional area to improve

the hydraulic performance of a single-channel pump *University of Science and Technology (in Korea)* ME Thesis
[8] JMP 6.0.0. 2005 The statistical discovery software. Version 6.0.0 SAS Institute Inc
[9] Deb K 2001 *Multi-objective optimization using evolutionary algorithm* (England, UK: John Wiley & Sons Inc.)
[10] MATLAB® 2004 *The language of technical computing*. Release 14 The Math Work Inc
[11] Kim J H 2015 Serialized development of a high-efficiency single-vane pump for waste treatment *Korea Institute of Industrial Technology* Annual report: JG150013
[12] Kim J H, Cho B M, Kim Y S, Choi Y S, Kim K Y, Kim J H and Cho Y 2016 Optimization of a single-channel pump impeller for wastewater treatment *International Journal of Fluid Machinery and Systems* **9** 4
[13] Kim J H, Cho B M, Choi Y S, Lee K Y, Peck J H and Kim S C 2016 Optimized reduction of unsteady radial forces in a single-channel pump for wastewater treatment *IOP Conf. Series: Earth and Environmental Science* 49